

Phase transitions in the $\text{Tl}_2\text{Ba}_2\text{CuO}_{6+\delta}$ superconductor

D. R. Pederzoli, G. M. Wltschek, and J. P. Attfield

Interdisciplinary Research Centre in Superconductivity, University of Cambridge, Madingley Road, Cambridge, CB3 0HE, United Kingdom

and Department of Chemistry, University of Cambridge, Lensfield Road, Cambridge, CB2 1EW, United Kingdom

H. Fuess

Technische Universität Darmstadt, Fachbereich Materialwissenschaft, Petersenstrasse 23, D-64287 Darmstadt, Germany

(Received 5 February 1998; revised manuscript received 8 April 1998)

Structural phase transitions in the ‘‘orthorhombic’’ form of the superconductor $\text{Tl}_2\text{Ba}_2\text{CuO}_{6+\delta}$ have been investigated by synchrotron x-ray powder diffraction. High-resolution studies show that oxygen rich compositions with T_c 's up to ≈ 70 K are monoclinic ($F112/m$ symmetry) with $90^\circ < \gamma < 90.2^\circ$ whereas slightly reduced samples with T_c 's of 70–90 K have orthorhombic $Fmmm$ symmetry. The peakwidths of the Bragg reflections show that the orthorhombic and monoclinic distortions induce microscopic strains in the ab plane. A high-temperature *in situ* synchrotron x-ray powder-diffraction experiment has been used to investigate the transitions between the monoclinic, orthorhombic, and thallium-deficient tetragonal forms of this material. The thermal variations of the macroscopic strains show that the 895 K monoclinic-orthorhombic phase transition, which is driven by loss of excess oxygen, is well described by Landau theory. However, the orthorhombic-tetragonal transition at 964 K, due to the loss of thallium oxide, shows a strong deviation from Landau behavior. A possible structural rearrangement of interstitial oxygen atoms is observed at 550–700 K. [S0163-1829(98)10233-3]

The $\text{Tl}_2\text{Ba}_2\text{CuO}_{6+\delta}$ (Tl-2201) superconductor is one of the most important materials for studies of intrinsic transport properties of high critical temperature superconductors,^{1,2} as it can be prepared as good quality tetragonal single crystals with low residual resistivities. The superconducting critical temperature (T_c) can be lowered from 90 K to below 4 K by addition of oxygen,³ allowing the overdoped regime of the superconducting phase diagram to be studied. As T_c is depressed by overdoping, the critical magnetic-field scale is rapidly decreased and the normal metallic state can be studied down to mK temperatures.² Recent studies on tetragonal Tl-2201 films have indicated the presence of pure anisotropic $d_{x^2-y^2}$ pairing symmetry with no contribution from isotropic s -wave pairing,^{4,5} emphasizing the important role of Tl-2201 in assisting the development of a theoretical model for high-temperature superconductivity.

As the first member of the $\text{Tl}_2\text{Ba}_2\text{Ca}_{n-1}\text{Cu}_n\text{O}_{4+2n}$ series, with $T_c(\text{max})=93$ K, $\text{Tl}_2\text{Ba}_2\text{CuO}_{6+\delta}$ has one of the highest T_c 's reported for compounds containing single CuO_2 layers.⁶ Unlike the other homologues which invariably display tetragonal symmetry, Tl-2201 is known to exhibit both tetragonal and orthorhombic forms, with physical properties varying from nonsuperconducting to superconducting with T_c up to 90 K. Flux-grown single crystals are always of the tetragonal form of Tl-2201, and as a result the orthorhombic variant has been rather less studied. Physical measurements⁷ and a resonant x-ray-diffraction study^{8,9} have shown that the two polymorphs possess slightly different compositions. The orthorhombic form is essentially thallium-stoichiometric $\text{Tl}_2\text{Ba}_2\text{CuO}_{6+\delta}$ whereas tetragonal Tl-2201 has a significant degree of Cu substitution at the Tl site with composition $(\text{Tl}_{1.9}\text{Cu}_{0.1})\text{Ba}_2\text{CuO}_{6+\delta}$. Recently, we have reported a monoclinic form of superconducting $\text{Tl}_2\text{Ba}_2\text{CuO}_{6+\delta}$, evidenced by

high-resolution time-of-flight neutron and synchrotron x-ray powder diffraction.¹⁰ This establishes Tl-2201 as a unique high- T_c material in displaying three distinct macroscopic structural symmetries as a function of small changes in composition. Here we report further high-resolution x-ray powder-diffraction studies on the monoclinic form, and a high-temperature *in situ* synchrotron x-ray powder-diffraction study of the changes in microscopic and macroscopic strains at the monoclinic-to-orthorhombic and orthorhombic-to-tetragonal phase transitions of this important superconductor. This *in situ* high-temperature diffraction study is unusual for thallium or mercury cuprate superconductors due to the difficulties caused by the volatility and toxicity of the heavy metals in these materials.

A bulk sample of polycrystalline monoclinic $\text{Tl}_2\text{Ba}_2\text{CuO}_{6+\delta}$ was prepared by conventional solid-state reaction.¹⁰ Portions of this ‘‘as-prepared’’ sample were individually annealed for 5 h under flowing Ar at temperatures of 200, 400, 450, 500, 550, 600, and 700 °C to systematically decrease the excess oxygen content δ , and a further portion was treated under 600 atm O_2 pressure at 600 °C to increase δ . Synchrotron x-ray powder-diffraction patterns of all samples were recorded at room temperature on the high-resolution diffractometer 9.1 at the Synchrotron Radiation Source, Daresbury, U.K. The wavelengths (see Table I) were calibrated using a NIST Si powder standard ($a = 5.43094 \text{ \AA}$). The profiles were fitted by the Rietveld method¹¹ using the GSAS package.¹² Observed, calculated, and difference plots for the x-ray profile of the 450 °C Ar-annealed sample are shown in Fig. 1. Diffraction peaks from traces of BaCO_3 and Tl_4O_3 (Ref. 13) were also observed in some of the profiles and were fitted in the refinements.

TABLE I. Superconducting critical temperatures (Ref. 10), cell data, and microstrains for monoclinic ($\gamma > 90^\circ$) and orthorhombic ($\gamma = 90^\circ$) $\text{Tl}_2\text{Ba}_2\text{CuO}_{6+\delta}$ samples with e.s.d.'s in parentheses.

Sample treatment	T_c (K)	a (Å)	b (Å)	c (Å)	γ (°)	Microstrain (%)	
						S_{\parallel}	S_{\perp}
600 atm, 600 °C O ₂ -annealed ^a		5.43890(9)	5.50414(10)	23.1569(4)	90.188(1)	0.09(1)	0.16(1)
As-prepared ^a		5.44746(14)	5.50517(15)	23.1556(5)	90.119(2)	0.08(1)	0.28(1)
200 °C Ar-annealed ^a	24	5.44663(17)	5.50424(18)	23.1517(6)	90.117(3)	0.10(1)	0.30(1)
400 °C Ar-annealed ^a	25	5.45092(14)	5.50119(15)	23.1645(5)	90.123(2)	0.07(1)	0.27(1)
450 °C Ar-annealed ^b	38	5.45590(9)	5.49672(9)	23.1901(3)	90.096(2)	0.09(1)	0.29(1)
500 °C Ar-annealed ^b	50	5.45842(12)	5.49889(13)	23.2003(4)	90.099(2)	0.10(1)	0.24(1)
550 °C Ar-annealed ^b	68	5.46289(13)	5.49777(14)	23.2127(4)	90.074(3)	0.08(1)	0.23(1)
600 °C Ar-annealed ^a	79	5.46457(12)	5.49509(13)	23.2174(5)	90	0.04(1)	0.25(1)
700 °C Ar-annealed ^a	90	5.46630(7)	5.49201(7)	23.2231(3)	90	0.02(1)	0.09(1)

^a $\lambda = 0.87194$ Å, $2\theta = 3 - 60^\circ$ in 0.01° steps.

^b $\lambda = 0.99902$ Å, $2\theta = 3 - 70^\circ$ in 0.01° steps.

A previous study¹⁰ showed that the Tl-2201 samples annealed in argon at temperatures ≤ 400 °C are monoclinic, but samples annealed ≥ 600 °C are orthorhombic, with the smallest monoclinic distortion corresponding to $\gamma = 90.12^\circ$ for the 400 °C Ar-annealed sample. The synchrotron x-ray diffraction data collected show that the 450, 500, and 550 °C Ar-annealed samples of Tl-2201 have monoclinic ($F112/m$) symmetry, with γ decreasing to 90.07° for the 550 °C sample. The observation of significant anisotropy in the Lorentzian broadening of the diffraction peaks has led us to reanalyze the previous and the recent data using an anisotropic lattice strain broadening function (1). Diffraction peaks were fitted by a numerical convolution of a constant Gaussian term and a variable Lorentzian function with full width at half maximum (FWHM) Γ_L given by^{14,15}

$$\Gamma_L = (Y + Y' \cos \phi) \tan \theta. \quad (1)$$

This expression allows for anisotropic lattice strain broadening through the Y' term, where ϕ is the angle between the chosen principal axis [001] and the reciprocal-lattice vector of the Bragg reflection. The results of these refinements are summarized in Table I. The refined Y and Y' parameters were converted to microstrains parallel (S_{\parallel}) and perpendicular (S_{\perp}) to the principal axis. An instrumental contribution,

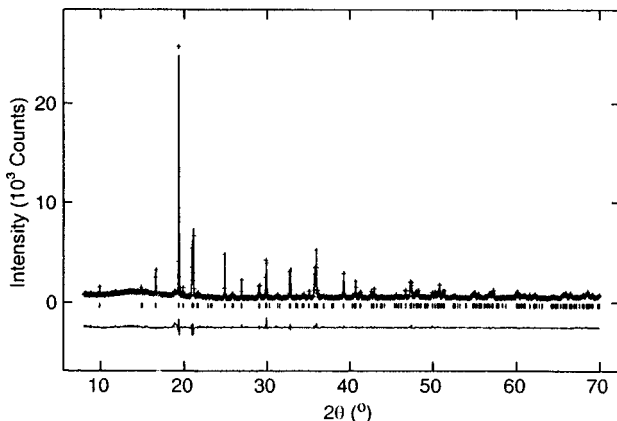


FIG. 1. Observed, calculated, and difference plot for monoclinic Tl-2201 (450 °C Ar-annealed) using a synchrotron x-ray wavelength of 0.87194 Å, with Bragg reflection positions marked.

determined by refinement of a silicon standard to be equivalent to a strain of 0.05%, has been subtracted from the values in Table I.

High-resolution synchrotron x-ray powder-diffraction studies have shown that samples annealed in argon at temperatures ≤ 550 °C are monoclinic, but samples annealed ≥ 600 °C are orthorhombic. Thus, the electronic properties of monoclinic Tl-2201 range from nonsuperconducting to superconducting with T_c up to ~ 70 K (Table I), whereas all orthorhombic Tl-2201 samples have T_c 's of $\sim 70 - 90$ K. From the variation in T_c with Ar-annealing temperature, it is clear that the extent of the monoclinic distortion is dependent upon the oxygen content. Determination of the excess oxygen content δ in $\text{Tl}_2\text{Ba}_2\text{CuO}_{6+\delta}$ is very difficult. Attempts to measure this accurately by thermogravimetry were unsuccessful due to traces of volatile thallium oxides in the samples. However, on the basis of an extensive neutron study by Wagner *et al.*,¹⁶ our results indicate a decrease in excess oxygen content δ from ≈ 0.13 in the as-prepared monoclinic sample to ≈ 0.03 in the 700 °C Ar-annealed orthorhombic sample. This is consistent with the observed change from overdoped nonsuperconducting behavior to superconducting with $T_c = 90$ K. Decreases in the microscopic strains determined from the Lorentzian components of the peakwidths of the Ar-annealed samples (Table I) also occur with the monoclinic to orthorhombic progression. A large excess strain in the ab plane S_{\perp} , relative to that in the c direction S_{\parallel} , is always observed, showing that the orthorhombic and monoclinic macrostrains lead to microstrains through twinning¹⁷ or other extended defects. S_{\parallel} for the monoclinic samples is significantly greater than for the orthorhombic phase, which may reflect the local strains due to their different interstitial oxygen contents. S_{\perp} does not show a simple dependence on crystal symmetry. The values for the as-prepared and samples annealed up to 600 °C in Ar are approximately constant but those for the high pressure and 700 °C Ar-annealed samples are much smaller. This suggests that the high-temperature annealing may have reduced the extent of twinning or other extended defects in these samples.

The as-prepared sample was also used for the *in situ* high-temperature synchrotron x-ray powder-diffraction experi-

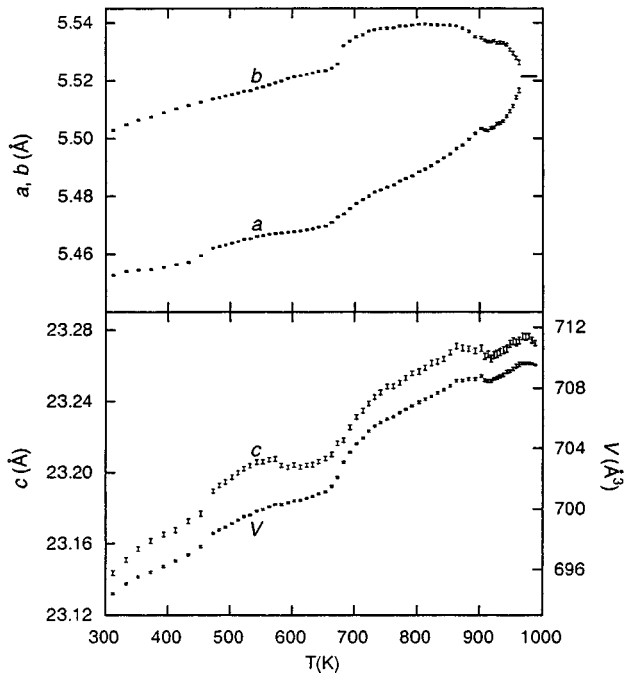


FIG. 2. Temperature dependence of cell parameters and volume in the range 313–988 K as derived from the *in situ* x-ray-diffraction study. The *a* parameter of the tetragonal phase ($T \geq 968$ K) is scaled by a factor of $\sqrt{2}$ for comparison with the *a* and *b* parameters of the orthorhombic material.

ment at HASYLAB Station B2, DESY, Germany. The diffractometer was used in Bragg-Brentano geometry with an INEL position-sensitive detector ($2\theta = 4$ to 124° in 0.03° intervals) for a time of 300 s at a wavelength of $\lambda = 1.7960$ Å. The sample was mounted in a thermocouple-controlled, resistively heated, furnace in an air atmosphere, and data were collected in the ranges 40–200 °C, 200–630 °C, and 630–750 °C with temperature increments of 20, 10, and 5 °C, respectively. The heating rate between temperatures was 2 °C/min and a time of 120 s was allowed for equilibration of the sample before data collection. The 2θ scale of the INEL detector was calibrated using an LaB_6 standard and the measured data were corrected using a least-squares cubic spline fit.¹⁸ Rietveld fits of the cell parameters were carried out using the GSAS package.¹² Part of the detector was obstructed by the furnace assembly so that data between $2\theta = 98$ and 108° were excluded from the refinements.

The high-temperature synchrotron x-ray powder-diffraction study enables the evolution of the monoclinic, orthorhombic, and tetragonal phases of Tl-2201 to be investigated *in situ*. Rietveld fits using the monoclinic $F112/m$ model were stable for data collected up to 893 K, but unstable thereafter, where the orthorhombic $Fmmm$ model was employed. The orthorhombic-tetragonal transition temperature was determined to be 968 K from the variation of the fitted¹⁹ FWHM of the 200/020 peak doublet with temperature. Fits to the data above this temperature were performed using tetragonal $I4/mmm$ symmetry. Sample decomposition, evidenced by the appearance of impurity peaks, was observed in diffraction patterns collected at temperatures above 993 K. The thermal variation of the refined cell parameters determined by Rietveld fitting is shown in Fig. 2.

The *in situ* high-temperature x-ray powder-diffraction study shows that up to ~ 670 K the steady increase in the *a*

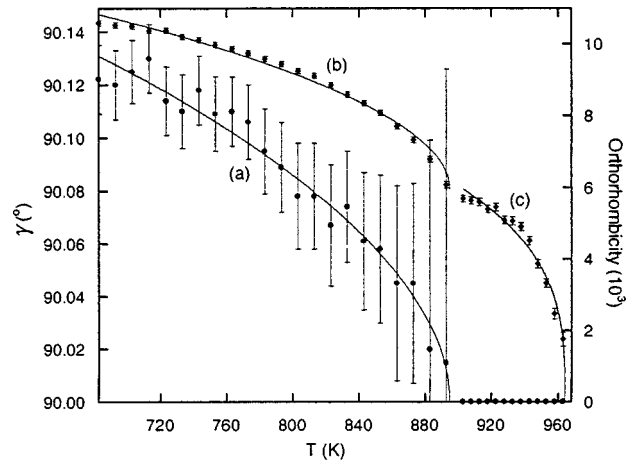


FIG. 3. Temperature dependence of γ (lower) and orthorhombicity (*o*) (upper) in the range 683–963 K as derived from the *in situ* x-ray-diffraction study. Three curve fits are shown: (a) $\gamma = \cos^{-1}[-2A(T_{m0} - T)^\beta]$ and (b) $o = A(T_{m0} - T)^\beta + o_{T_{m0}}$, model the monoclinic-orthorhombic transition with $T_{m0} = 895(3)$ K and $\beta = 0.5$ within experimental error, and (c) $o = A(T_{ot} - T)^\beta$ for the orthorhombic-tetragonal transition with $T_{ot} = 964(1)$ K and $\beta = 0.31(3)$. The error bars correspond to one e.s.d.

and *b* cell parameters is attributable to normal thermal expansion effects (Fig. 2). However, at 550–700 K there is an anomalous reduction in *c* and the cell volume compared to the trend above and below this range. This is unlikely to be due to a further uptake of oxygen, as the sample was slow-cooled under oxygen after synthesis, but may be due to the formation of a more ordered structure, possibly a rearrangement of interstitial oxygen within the Ti_2O_2 bilayer. Evidence for the filling of at least two oxygen sites within the TlO layers has recently been reported,¹⁶ and electron microscopy has also revealed a superstructure in orthorhombic Tl-2201 that might be due to this type of ordering.¹⁷ No superstructure peaks are discernible in our data, but this may reflect the low occupancy and weak x-ray scattering power of the interstitial oxygen. The sharp increases in *a*, *b*, and *c* at 670–750 K are consistent with a subsequent disordering and initial loss of the interstitial oxygen from the structure, which coincides with the rise of T_c with Ar-annealing temperature (Table I).

The monoclinic angle, γ , and the orthorhombicity, $o = 2(b - a)/(b + a)$, characterize the macroscopic strains within the lattice. The *in situ* high-temperature x-ray powder-diffraction study reveals a critical variation in γ and the excess orthorhombicity at the monoclinic-orthorhombic phase transition (Fig. 3). To determine whether this variation is in accordance with the Landau theory of second-order phase transitions, we take the e_{12} component of the spontaneous strain tensor²⁰ to be proportional to the order parameter, since this component corresponds to the strain induced by the angular distortion of the *ab* plane. If the lattice parameters of the lower symmetry phase are *a*, *b*, *c*, α , β , γ and those of the higher symmetry phase are a_0 , b_0 , c_0 , α_0 , β_0 , γ_0 , then the monoclinic strain, $\epsilon_m = |e_{12}|$, is given by²¹

$$\epsilon_m = -1/2(a \cos \gamma / a_0 \sin \gamma_0 - b \cos \gamma_0 / b_0 \sin \gamma_0), \quad (2)$$

where the b axis has a common direction in both phases. For the monoclinic-orthorhombic transition, this reduces to

$$\varepsilon_m = -a \cos \gamma / 2a_0, \quad (3)$$

where $a_0(T)$ over the range of the monoclinic-orthorhombic transition describes the variation of the a -lattice parameter of the orthorhombic material had the transition not taken place. However, since the change in the a parameter over the range 683–903 K amounts to less than 1%, the factor a/a_0 has a negligible effect on the expression for ε_m , and may be approximated to unity.

Landau theory predicts $\varepsilon_m \propto (T_0 - T)^{1/2}$ for temperatures below the transition temperature T_0 . At least-squares curve fit to the data [Fig. 3(a)] of the form: $\varepsilon_m = A(T_{\text{mo}} - T)^\beta$ yields a monoclinic-orthorhombic transition temperature $T_{\text{mo}} = 895(3)$ K with a critical exponent $\beta = 0.53(4)$. A least-squares fit of the variation of the excess orthorhombic strain described by the orthorhombicity, $o = A(T_{\text{mo}} - T)^\beta + o_{T_{\text{mo}}}$ with the latter value of T_{mo} (where $o_{T_{\text{mo}}}$ is the residual orthorhombicity at the monoclinic-orthorhombic transition) yields $\beta = 0.52(2)$ [Fig. 3(b)]. Both the fitted β values are within error of 0.5 showing that the monoclinic-orthorhombic transition is well described by Landau theory and is not driven by a large change in chemical composition.

The variation of orthorhombic strain with temperature in the region 903–963 K, below the orthorhombic-tetragonal transition, is not described by Landau theory. A least-squares fit of the form: $o = A(T_{\text{ot}} - T)^\beta$, yields an orthorhombic-tetragonal transition temperature $T_{\text{ot}} = 964(1)$ K and $\beta = 0.31(3)$ [Fig. 3(c)]. This transition is driven by the substitution of Cu for Tl with loss of Tl_2O_3 [as $\text{Tl}_2\text{O} + \text{O}_2$ (Ref. 22)] and to balance stoichiometry, an unobserved exsolution of barium oxide. This significant change in chemical composition may account for the non-Landau behavior at the transition.

Despite the use of larger F -centered crystallographic cells for the orthorhombic and monoclinic forms, all three phases of Tl-2201 can be represented by I -centered cells. The tetragonal form has $a = b$ and $\gamma = 90^\circ$ with $a \approx 3.864$ Å. The orthorhombic phase results from an angular distortion in the ab plane giving $a = b$, $\gamma > 90^\circ$ (e.g., $a = 3.874$ Å, $\gamma = 90.27^\circ$ for the orthorhombic, 700 °C Ar-annealed sample). An increase in the angular distortion of this body-centered cell accompanies the elongation of the b parameter relative to a , ($a \neq b$, $\gamma > 90^\circ$) which occurs in the monoclinic phase (e.g., $a = 3.868$ Å, $b = 3.876$ Å, $\gamma = 90.60^\circ$ for the monoclinic, as-prepared sample).

In conclusion, the amount of excess oxygen in Tl-stoichiometric $\text{Tl}_2\text{Ba}_2\text{CuO}_{6+\delta}$ controls both the crystal symmetry and electronic properties. Oxygen-rich compositions with T_c 's up to ≈ 70 K are monoclinic with $90^\circ < \gamma < 90.2^\circ$, whereas slightly reduced samples with T_c 's of 70–90 K are orthorhombic. The phase-transition temperatures depend upon oxygen partial pressure. The monoclinic to orthorhombic transition occurs in the range 550–600 °C under an argon atmosphere and at 620 °C in air, and is well described by Landau theory. The orthorhombic to tetragonal transition shows a strong deviation from this behavior due to loss of Tl_2O_3 and substitution of Cu at the Tl site to give the Tl-deficient tetragonal superconductor, $(\text{Tl}_{1.9}\text{Cu}_{0.1})\text{Ba}_2\text{CuO}_{6+\delta}$. The thermal variations of the cell parameters suggest a possible structural rearrangement of interstitial oxygen atoms in the monoclinic phase at 280–430 °C.

We thank Dr. G. Bushnell-Wye and A. M. T. Bell for assistance with data collection and Dr. S. A. T. Redfern for useful discussions. We acknowledge the Engineering and Physical Sciences Research Council for the provision of beam time at Daresbury and for financial support for D.R.P., and the British Council for an ARC award.

- ¹T. Manako, Y. Kubo, and Y. Shimakawa, Phys. Rev. B **46**, 11 019 (1992).
- ²A. P. Mackenzie, S. R. Julian, G. G. Lonzarich, A. Carrington, S. D. Hughes, R. S. Liu, and D. C. Sinclair, Phys. Rev. Lett. **71**, 1238 (1993).
- ³T. Manako, Y. Kubo, Y. Shimakawa, and H. Igarashi, Phys. Rev. B **43**, 7875 (1991).
- ⁴C. C. Tsuei, J. R. Kirtley, M. Rupp, J. Z. Sun, A. Gupta, M. B. Ketchen, C. A. Wang, Z. F. Ren, J. H. Wang, and M. Bhushan, Science **271**, 329 (1996).
- ⁵C. C. Tsuei, J. R. Kirtley, Z. F. Ren, J. H. Wang, J. H. Raffy, and Z. Z. Li, Nature (London) **387**, 6632 (1997).
- ⁶Z. Z. Sheng and A. M. Hermann, Nature (London) **332**, 55 (1988).
- ⁷Y. Shimakawa, Physica C **204**, 247 (1993).
- ⁸J. P. Attfield, M. A. G. Aranda, and D. C. Sinclair, Physica C **235**, 965 (1994).
- ⁹M. A. G. Aranda, J. P. Attfield, D. C. Sinclair, and A. P. Mackenzie, Phys. Rev. B **51**, 12 747 (1995).
- ¹⁰D. R. Pedersolli, G. M. Wltschek, and J. P. Attfield, Chem. Commun. (Cambridge) **5**, 435 (1997).
- ¹¹H. M. Rietveld, J. Appl. Crystallogr. **2**, 65 (1969).
- ¹²A. C. Larson and R. B. Von Dreele, Los Alamos National Laboratory Report No. LA-UR-86-748 (1987).
- ¹³R. Marchand and M. Tournoux, C. R. Hebd. Seances Acad. Sci. C **277**, 863 (1973).
- ¹⁴C. J. Howard, J. Appl. Crystallogr. **15**, 615 (1982).
- ¹⁵P. Thompson, D. E. Cox, and J. B. Hastings, J. Appl. Crystallogr. **20**, 79 (1987).
- ¹⁶J. L. Wagner, O. Chmaissem, J. D. Jorgensen, D. G. Hinks, P. G. Radaelli, B. A. Hunter, and W. R. Jensen, Physica C **277**, 170 (1997).
- ¹⁷E. A. Hewat, P. Bordet, J. J. Capponi, C. Chaillout, J. Chenavas, M. Godhino, A. W. Hewat, J. L. Hodeau, and M. Marezio, Physica C **156**, 375 (1988).
- ¹⁸Data from the INEL detector were calibrated using v1.05 of the ENFRA-GUFI package. R. E. Dinnebier, Ph.D. thesis, University of Heidelberg, 1993.
- ¹⁹Least-squares peak fitting was performed using v1.2 of the WINFIT program; S. Krumm, Mater. Sci. Forum **228-231**, 183 (1996).
- ²⁰K. Aizu, J. Phys. Soc. Jpn. **28**, 706 (1970).
- ²¹J. L. Schlenker, Acta Crystallogr., Sect. A: Cryst. Phys., Diffr., Theor. Gen. Crystallogr. **34**, 52 (1978).
- ²²D. Cubicciotti and F. J. Keneshea, J. Phys. Chem. **71**, 808 (1967).